Catal Lett (2009) 131:624–631
DOI 10.1007/s10562-009-9981-3

Nature of Phthalates as Internal Donors in High Performance $MgCl_2$ Supported Titanium Catalysts

Umesh Makwana · Dhananjay G. Naik · Gurmeet Singh · Vallabhbhai Patel · Harshad R. Patil · Virendra K. Gupta

Received: 2 March 2009 / Accepted: 14 April 2009 / Published online: 23 May 2009

Abstract High performance $MgCl_2$ supported titanium catalyst having diisobutyl phthalate (DIBP) as internal donor has been synthesized. The organic components present in the catalyst have been studied through FTIR, 1D and 2D NMR spectroscopy. The results indicate presence of diethyl phthalate also in addition to DIBP. WAXD analysis has been done to study the features of $MgCl_2$ crystallites. Impact of donor components on the catalyst preparation leading to reaction pathways and performance for propylene polymerization has been evaluated.

Keywords Ziegler–Natta catalyst · Internal donors · Magnesium dichloride · NMR spectroscopy

1 Introduction

High performance $MgCl_2$ supported Ziegler–Natta catalysts have played dominant role in industrial polyolefin production [1–5] by providing high productivity and stereoregularity [6–11]. Internal donors play the pivotal role in controlling productivity and stereo-specificity of these catalysts [12–18]. The evolution of consecutive generations of $MgCl_2$ supported titanium catalysts has been achieved through selection of internal donors. Spitz et al. [19] recently reported that internal donors might not have any direct role in the active site formation. Thus the role of internal donors for stabilizing $MgCl_2$ crystallites and blocking non-stereospecific/low productive sites become very critical. Hence understanding of organic components present in the catalysts becomes crucial for comprehensive knowledge of the catalyst chemistry.

$MgCl_2$ revolutionized the field of Ziegler–Natta catalysts by providing support to titanium chloride species, the active catalyst, thereby increasing catalytic productivity and endowing with a tool for controlling morphology of catalyst and polypropylene as the end product. Active $MgCl_2$ has small crystallite size and lateral cuts having four and five coordinated Mg cations in comparison to six coordinated Mg cations in the bulk, these lateral cuts acts as the support to $TiCl_4$ and donors [20–24]. The active $MgCl_2$ can be obtained from mechanical route, by ball milling $MgCl_2$ in presence of $TiCl_4$ and Lewis base, from chemical route by elimination of Lewis base from $MgCl_2$.(Lewis base)$_x$ adducts and during catalyst preparation from magnesium ethoxide [25, 26]. The conversion of magnesium precursor to catalyst results in active $MgCl_2$ and in situ generation of other phthalate esters and phthaloyl chloride species. The presence of –COCl species, a reaction side product, has been observed from FTIR spectral studies. DIBP, a Lewis base, binds to Lewis acid sites (Mg^{2+} ions on lateral cuts) on the $MgCl_2$ matrix. Complex formation between DIBP and Mg^{2+} ions can be studied through FTIR spectroscopy providing information regarding their bonding modes [26–29].

NMR spectroscopy has been applied in Zielger–Natta catalyst science for understanding interaction of various components. Busico et al. [5] reported the high resolution magic-angle-spinning ^1H NMR studies of active site surfaces of $MgCl_2$ supported Ziegler–Natta catalysts. Kissin et al. [29] reported the application of 13C NMR spectroscopy for analyzing the interactions of triethyl aluminum (TEAl) with DIBP and silyl ethers. Ikeuchi et al. [30]

U. Makwana · D. G. Naik · G. Singh · V. Patel · H. R. Patil · V. K. Gupta (✉)
Catalyst & Material Reliance Technology Center, Reliance Industries Ltd., Hazira Complex, Surat, Gujarat 394510, India
e-mail: Virendrakumar_Gupta@ril.com

reported NMR spectroscopic studies on the mixture of TEAl and aminosilanes.

In this study, NMR spectroscopy has been applied to understand the structure and quantification of organic species present in the catalyst. DEPT spectroscopy allows differentiating methyl, methylene and methine nuclei resonances. 1D homonuclear (^{1}H–^{1}H) and heteronuclear (^{1}H–^{13}C) correlation spectroscopy allowed building of skeleton framework of organic molecules. 2D NMR spectroscopy in conjugation with 1D NMR spectroscopy allowed the comprehensive assignments of NMR spectra and structure elucidation of organic components. Quantification of the organic components has been done by ^{1}H spectroscopy supported by HPLC. To the best of our knowledge, application of NMR spectroscopy for understanding organic components in high performance $MgCl_2$ supported titanium catalysts has not been reported. The reaction pathway for the synthesis of organic components during catalyst preparation has been explored. Catalyst has been subjected to WAXD analysis for characterizing the $MgCl_2$ matrix structure.

2 Experimental

2.1 Synthesis and Materials

All experimental manipulations were carried out in nitrogen atmosphere using dry-box and Schlenk line techniques. For the Catalyst-1 synthesis, magnesium ethoxide was treated with titanium tetrachloride and chlorobenzene mixture in the presence of diisobutyl phthalate as internal donor at elevated temperature. Further treatment of titanium tetrachloride and chlorobenzene mixture was given followed by isolation of solid catalyst by hexane washing [31]. For the Catalyst-2 and Catalyst-3 synthesis phthaloyl chloride was added in 0.5:1 and 1:1 mol ratio with respect to DIBP, respectively.

2.2 FTIR Spectroscopy

Nujol mull of catalysts were prepared and loaded on KBr discs in glove box and transferred in airtight container to FTIR instrument. FTIR analysis was performed on Perkin–Elmer spectrum GX instrument with 2 cm^{-1} resolution and 32 scans under nitrogen flow.

2.3 NMR Spectroscopy

1D and 2D NMR spectra were recorded on Bruker DPX-400 spectrometer in methanol-d4. Weighed amount of catalyst samples and 1,1,2,2-tetrachloroethane (TCE) as internal standard (for quantitative measurements) were dissolved in methanol-d4 and transferred to NMR tube in nitrogen bag. ^{1}H and ^{13}C measurements were made at frequencies of 400 and 100 MHz, respectively, and calibrated with respect to the solvent signal. For quantitative estimations ^{1}H NMR spectra were recorded with 10 s delay time, 32 K data points were accumulated for 16 successive scans. A total of 4,000 scans were accumulated for ^{13}C{^{1}H} NMR spectra with a relaxation delay of 2 s. Distortionless enhancement by polarization transfer (DEPT) experiments were carried out using the standard pulse sequence with 2 s delay time. Heteronuclear multiple quantum coherence (HMQC) experiments were recorded using the standard pulse sequence from the Bruker software library. 64 scans were averaged for each of 512 increments along t_1 and 2,048 data points in t_2. The HMQC experiment was optimized for $^1J_{CH} = 145$ Hz. TOCSY (Total Correlation spectroscopy) experiments were performed using standard pulse sequence. 64 scans were accumulated for 512 experiments with 2 s delay time.

2.4 HPLC Measurements

HPLC measurements were carried on a Perkin Elmer Series 200 HPLC instrument system using Brownlee C-18, 5 μm, 250 mm × 4.6 mm HPLC analytical column. The mobile phase was consisting of 65/35 distilled water/methanol (HPLC grade, Labort, India)/distilled water. The column was eluted at a flow rate of 1.0 mL min^{-1} at 35 °C with UV detector working wavelength of 230 nm.

2.5 WAXD Measurements

Wide angle X-ray diffraction: X-ray diffraction measurements were carried on Bruker AXS, D8 Advance X-ray diffractometer. The catalyst samples were placed on the zero background, X-ray transparent airtight sample holder in the glove box in nitrogen environment to perform measurements in inert atmosphere. The step size in WAXD measurements was 0.02 degrees and the time per step 12 s.

2.6 Propylene Polymerization

Cocatalyst (triethyl aluminium) and catalyst were added to maintain the Al:Ti in 250:1 molar ratio to jacketed reactor containing hexane as solvent. Cyclohexylmethyl dimethoxysilane was added as external donor with 1:30 molar ratio with respect to cocatalyst. Propylene pressure of 5 kg cm^{-2} was maintained and hydrogen was added as chain terminating agent. Polymerization was carried out for 1 h at 70 °C, afterwards polypropylene was isolated and vacuum dried. Productivity of the catalysts was calculated from the polypropylene yield (kg) to the catalyst amount

Table 1 Characteristics of synthesized $MgCl_2$ supported titanium catalysts

Catalyst	Analysis (wt%)					
	Ti	Cl	Mg	Hexane (NMR)	DIBP (HPCL)	DEP (HPLC)
1	2.9	60	18.5	2.7	11.5	1.1
2	3.2	61	18.0	1.7	7.2	2.3
3	3.3	61	17.8	2.5	6.3	2.7

(g). Polypropylene samples were extracted with boiling xylene in Soxlet apparatus. Isotacticity index (II) was measured as wt% of xylene insoluble for each PP sample (Table 1).

3 Results and Discussion

3.1 Reaction Pathway

Catalyst synthesis from magnesium ethoxide by the reaction with $TiCl_4$ in the presence of DIBP (internal donor) follows complex reaction pathway [31]. There are several chemical (Scheme 1) and physical changes going on simultaneously. Magnesium ethoxide (1) is getting converted to $MgCl_2$ (3) by reacting with $TiCl_4$ (2), involving chemical transformation and simultaneous getting reorganized in the form of $MgCl_2$ crystallites involving reorientation of magnesium coordinates with formation of $TiCl_3(OCH_2CH_3)$ (4).

$TiCl_4$, a Lewis acid, acts as a catalyst for substitution reactions leading to the formation of other pthalate esters in the presence of ethoxide species and phthaloyl chloride, which being Lewis bases also act, as internal donors. The proposed pathway for the formation of these species can be been explained on the basis of Scheme 1 (for simplification, free donor molecules have been shown). $TiCl_4$ reacts with DIBP (5) to form product 7, which in the presence of excess amount of $TiCl_4$ gives phthaloyl chloride (8). Product 7 on reacting with 4 results in isobutyl ethyl phthalate (9) formation and phthaloyl chloride on reacting with 4 results in the formation of diethylphthalate (10). Internal donors (ID), Scheme 1, (5), (7), (8), (9) and (10) (Lewis bases) and $TiCl_4$ get coordinated to $MgCl_2$ matrix, forming the active catalyst. Coordination of phthaloyl chloride and DIBP with $MgCl_2$ has been studied through FTIR spectroscopy. The complex mixture of phthalate esters has been identified and quantified using 1D and 2D NMR spectroscopy assisted by HPLC. The structural features of $MgCl_2$ crystallites have been studied through WAXD analysis.

3.2 Complexes on $MgCl_2$ Matrix

DIBP, a Lewis base, coordinates with Lewis acid sites on $MgCl_2$ matrix through carbonyl oxygen having high electron density. Complex formation is best studied through FTIR spectroscopy as >C=O stretching frequency is highly sensitive to coordination of oxygen atom with Mg ions [26–29]. For Catalyst-1, the shift in >C=O stretching band from DIBP to catalyst, where DIBP is coordinated with Mg ions of $MgCl_2$ matrix, is evident from Fig. 1a with the shift in band from 1,728 cm^{-1} to a broad peak at 1,687 cm^{-1}. The broad peak is representation of several superimposing IR bands, corresponding to different complexes of DIBP with $MgCl_2$ and contribution from complexes of other phthalate esters. The different complexes of DIBP with $MgCl_2$ are due to the coordination of DIBP to 4 and 5 coordinated Mg ions on (110) and (104) lateral cuts, respectively, and to 3 coordinated Mg ions on the edges and corners of $MgCl_2$ crystallites.

Other IR bands of interest are C–O–C symmetric and asymmetric stretching vibrations at 1,151 and 1,311 cm^{-1}. O–C=O symmetric and asymmetric stretching vibrations appear at 936 and 1,082 cm^{-1}. The DIBP-$TiCl_4$ complex has >C=O stretching band at 1,647 cm^{-1}, which is overlapping with the broad >C=O band. The bands at higher frequencies 1758, 1832 and 1861 cm^{-1} are attributed to the complex between $MgCl_2$ and phthaloyl chloride species (–COCl), which get formed during catalyst synthesis at high temperatures.

For the synthesis of Catalyst-2 and Catalyst-3, phthaloyl chloride was added during catalyst preparation and it should have higher concentration of phthaloyl chloride in comparison to Catalyst-1. On comparing the IR spectra for Catalyst-1, Catalyst-2 and Catalyst-3, Fig. 1a, b and c, respectively, it's evident that the IR bands corresponding to –COCl at 1758, 1832 and 1861 cm^{-1} have higher relative intensities for Catalyst-2 and Catalyst-3. The relative ratio of IR band for DIBP at 1,687 cm^{-1} to IR band for COCl at 1,758 and 1,861 cm^{-1} is 11 and 41 for Catalyst-1; 5 and 11 for Catalyst-2; 2 and 4 for Catalyst-3, indicating increase in phthaloyl chloride species for Catalyst-2 and Catalyst-3.

FTIR bands indicate the presence of DIBP-$MgCl_2$ complexes, DIBP-$TiCl_4$ complex and phthaloyl chloride-$MgCl_2$ complexes. The presence of phthalate esters other than DIBP can not be studied through FTIR spectroscopy only and has been substantiated by NMR spectroscopy.

3.3 Phthalate Esters Analysis

^1H NMR spectrum of Catalyst-1 is given in Fig. 2, with insets showing the respective expanded regions. The spectrum can be divided into four regions, 0.7–2.1, 3.2–4.4 ppm, sharp peak at 6.5 and 7.5–7.8 ppm. A number of

Scheme 1 Proposed reaction scheme for chemical transformations of donors during catalyst synthesis

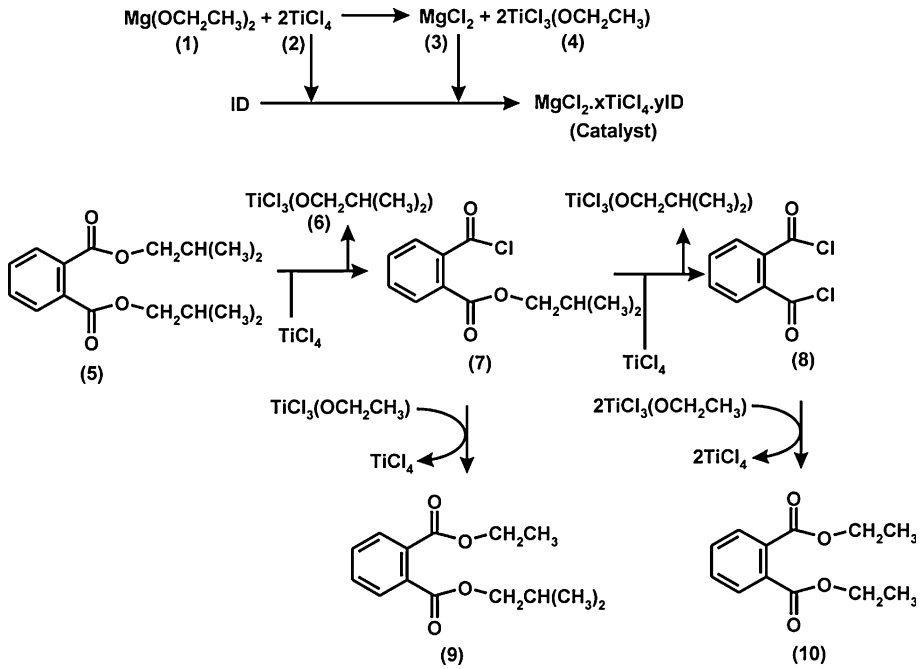

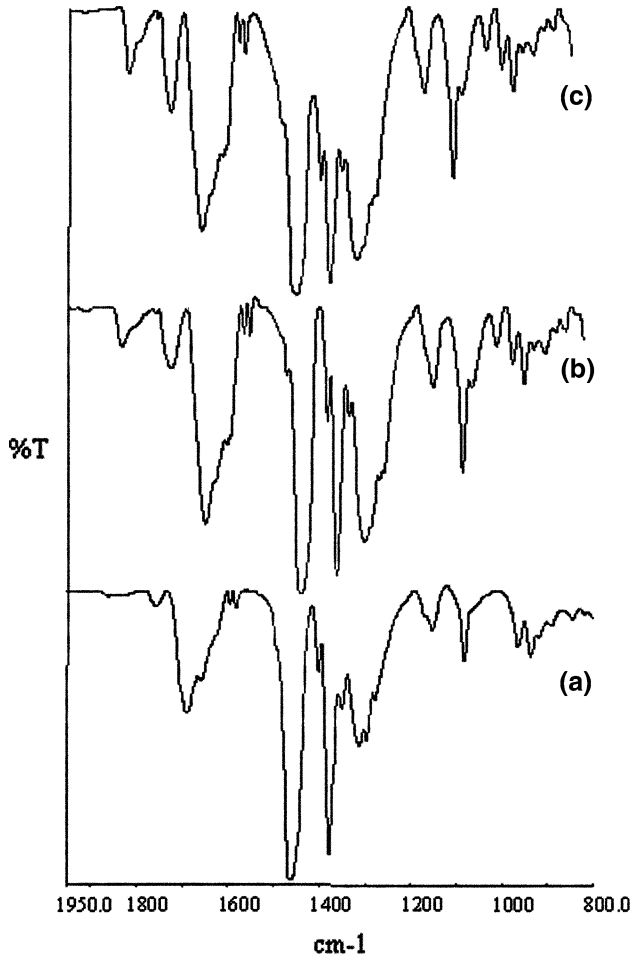

Fig. 1 FTIR spectrum of *a* Catalyst-1, *b* Catalyst-2 and *c* Catalyst-3

resonances indicate presence of multiple organic components. Peak at 3.31 is assigned to methanol and peak at 6.54 to 1,1,2,2-tetrachloroethane. The set of resonances at 7.5–7.8 ppm are assigned to the aromatic ring protons of phthalic esters. Assignments of the remaining resonances have been made using ^{13}C, DEPT and 2D correlation NMR spectroscopy.

$^{13}C\{^{1}H\}$, DEPT-90 and DEPT-135 spectra of Catalyst-1 are given in Figs. 3a, 4a and b, respectively. $^{13}C\{^{1}H\}$ is characterized by the presence a large number of resonances, which have been further resolved using DEPT spectroscopy. DEPT-90 spectrum, which is selective to methine resonances, has two peaks at 28.67 and 75.75 ppm, indicating presence of two methine groups. Methylene resonances are resolved through DEPT-135 spectroscopy, where the methyl and methane resonances are in positive phase and methylene resonances are in negative phase. DEPT-135 spectrum shows the presence of five methylene resonances at 23.4, 32.4, 58.14, 62.5 and 72.5 ppm.

Comprehensive assignments of ^{1}H and $^{13}C\{^{1}H\}$ NMR spectrum have been done from HMQC and TOCSY spectrum, Figs. 5 and 6, respectively, by building the framework of organic components. The proton at 0.83 ppm shows cross-peak 1 with methyl carbon at 14.35 and cross-correlation peak I at 1.22 ppm. The proton at 1.22 ppm shows two cross-peaks, 5 and 7, with methylene carbons at 23.41 and 32.43 ppm indicating presence of hydrocarbon component with three types of carbon nuclei. The organic component is hexane, which was used for final catalyst washing.

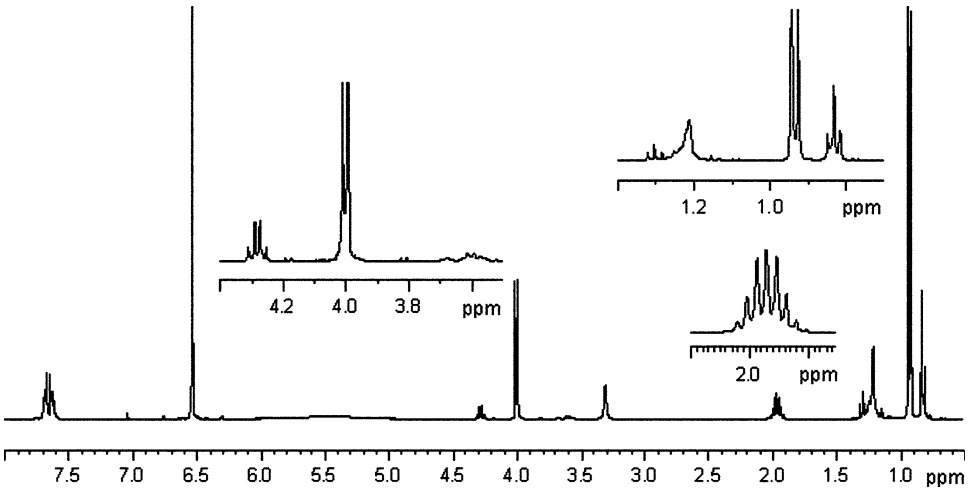

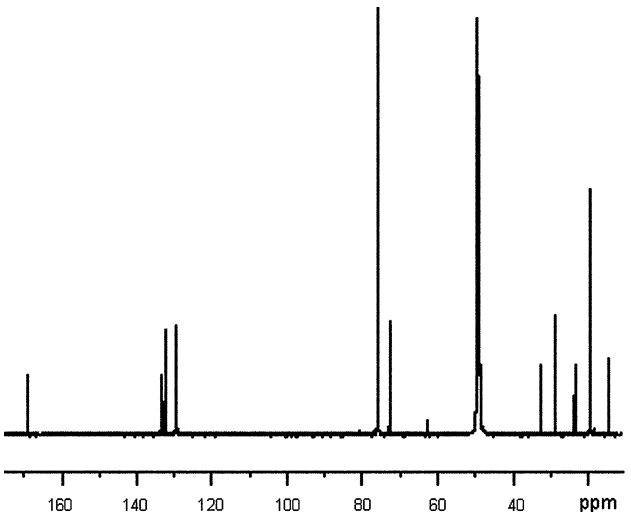

Fig. 3 $^{13}C\{^{1}H\}$ NMR spectrum of Catalyst-1

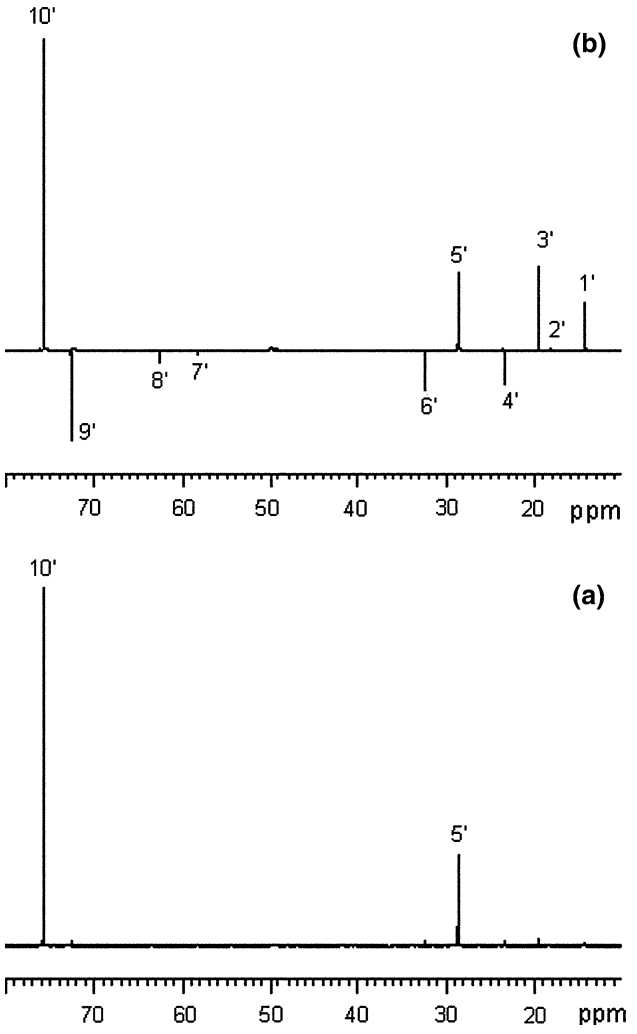

Fig. 4 **a** DEPT-90 and **b** DEPT-135 NMR Spectrum of Catalyst-1

The proton at 0.94 ppm shows cross-correlation peaks II and III with protons at 1.97 and 4.01 ppm, respectively, and cross-peak 4 to methyl carbon at 19.39 ppm. Thus, organic component with coupled system of three protons is present. The protons at 1.97 and 4.01 ppm show cross-peaks 6 and 11 with methine carbon at 28.67 ppm and methylene carbon at 72.54 ppm, respectively. The high chemical shift of 4.01/72.54 methylene group point that it is bonded to oxygen atom and the doublet ^{1}H peak indicates that it is coupled to CH group. ^{1}H resonance of CH group with heptad multiplicity indicates that it is bonded to two CH_3 groups. Hence the structure of the organic component is isobutyl group $\{-CH_2CH(CH_3)_2\}$, that of the isobutyl group of phthalic ester $\{-CO_2CH_2CH(CH_3)_2\}$. Cross-correlation peak VI is due to coupling of methine and methylene protons.

Cross-correlation peak IV is due to coupling of protons with chemical shifts of 1.15 and 3.60 ppm. The proton having triplet at 1.15 ppm has cross-peak 3 with methyl carbon at 18.24 ppm and proton at 3.60 ppm has cross-peak 9 with methylene carbon at 58.14 ppm. The chemical shift values and backbone structure indicate the presence of

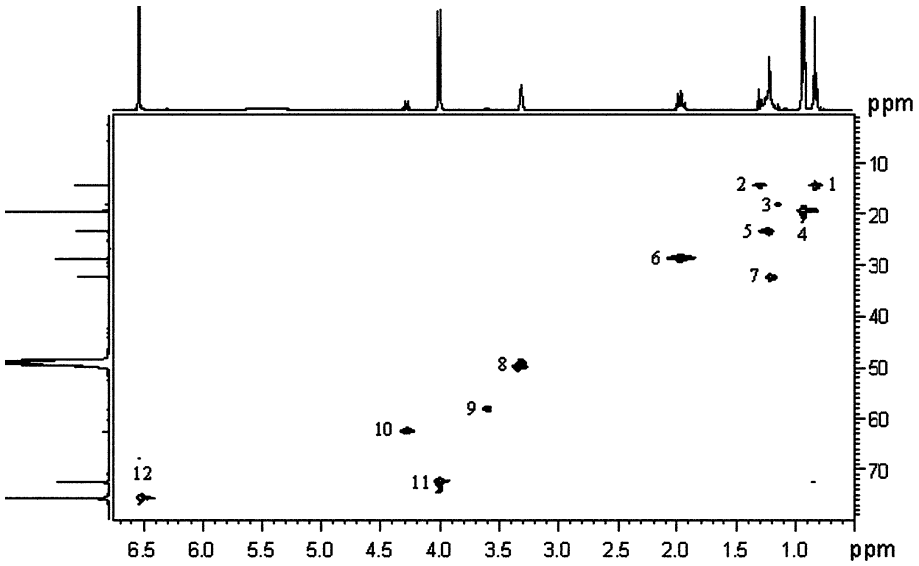

Fig. 5 2D HMQC spectrum of Catalyst-1

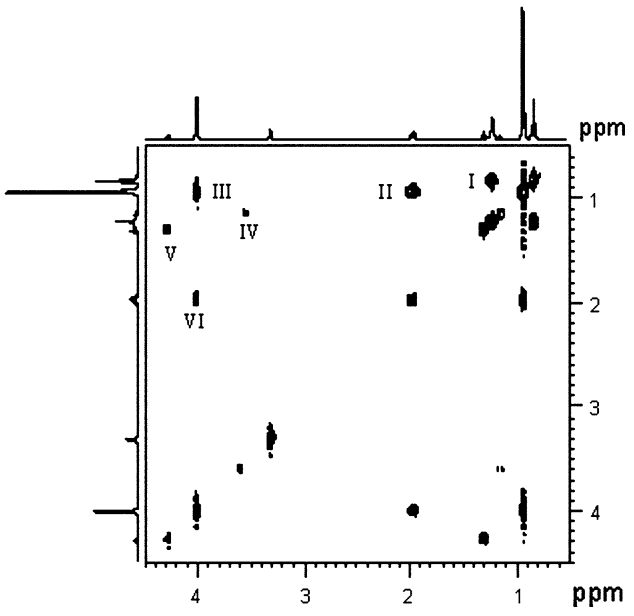

Fig. 6 2D TOCSY spectrum of Catalyst-1

ethoxide, from component (4) in Scheme 1, present in very low concentration, which forms during catalyst synthesis.

Proton with triplet at 1.30 ppm Cross-correlation peak V at 1.30/4.28 ppm is from the coupling of protons characterized by triplet (1.30 ppm) and quartet (4.28 ppm). The protons at 1.30 and 4.28 ppm in turn are coupled to methyl carbon at 14.35 ppm (cross-peak 2) and methylene carbon at 62.53 ppm (cross-peak 10). This leads to the conclusion that ethyl group is present. High chemical shift 62.53/4.28 of methylene group indicates presence of $–CO_2CH_2CH_3$ group of phthalic ester. This is formed during catalyst synthesis as given in Scheme 1 with $Mg(OEt)_2$ as the ethoxide source and $TiCl_4$ as transesterification agent enabling the synthesis of ethyl phthalate esters.

The assignments of HSQC and TOCSY spectrum are given in Table 2 and 3, respectively. Hexane, isobutyl phthalate esters, ethyl phthalate esters and ethoxide are the organic components identified from the comprehensive NMR spectral analysis. Assigned ^1H spectrum allows the quantification of various organic components present in the catalyst. Integral intensities corresponding to the following well resolved resonances (1) CH_2 of isobutyl phthalate ester, (2) CH_2 of ethyl phthalate, (3) CH_3 of hexane, and (4) CH_2 of ethoxide were calculated and respective organic components were quantified using the integral intensity of 1,1,2,2 tetrachloroethane resonance at 6.54 ppm which has been added as internal standard for quantification. This enabled to quantify the main organic components present in the catalyst system and residual hexane from washing of the catalysts.

The wt% of $–CO_2CH_2CH(CH_3)_2$/$–CO_2CH_2CH_3$ calculated from ^1H NMR spectra are 8.6/0.9, 5.7/1.8, 5.0/2.2 for Catalyst-1, Catalyst-2 and Catalyst-3, respectively. Considering that these groups belong to DIBP and DEP only, than the wt% for DIBP and DEP should be 11.9 and 1.6 in comparison to 11.5 and 1.1 as determined from HPLC for Catalyst-1. The difference in NMR and HPLC quantitative analysis indicates that the $–CO_2CH_2CH(CH_3)_2$ and $–CO_2CH_2CH_3$ groups are contributing to some other component, which can be the product 9 (Scheme 1). To further substantiate the reaction pathway proposed in Scheme 1, Catalyst-2 and Catalyst-3 were prepared with the addition of phthaloyl chloride during catalyst synthesis. It was envisaged that if the formation of DEP is through phthaloyl chloride (8), than with its addition the DEP concentration should increase in catalyst. It was indeed

Table 2 Assignments of the ^{13}C and ^{1}H resonances from the 2D HSQC spectrum and corresponding peaks in DEPT 90 and DEPT 135 Spectrum

Cross-peak No.	Cross-peak assignment	Cross-peak position (ppm)	Corresponding peak in DEPT spectra
1	Methyl of hexane	14.35/0.83	1′
2	Methyl of $–CO_2CH_2CH_3$	14.35/1.30	1′
3	Methyl of ethanol	18.24/1.15	2′
4	Methyl of $–CO_2CH_2CH(CH_3)_2$	19.39/0.94	3′
5	Methylene of hexane	23.41/1.23	4′
6	Methine of $–CO_2CH_2CH(CH_3)_2$	28.67/1.97	5′
7	Methylene of hexane	32.43/1.21	6′
8	Methyl of methanol	49.15/3.31	–
9	Methylene of ethanol	58.14/3.60	7′
10	Methylene of $–CO_2CH_2CH_3$	62.53/4.28	8′
11	Methylene of $–CO_2CH_2CH(CH_3)_2$	72.54/4.01	9′
12	Methine of 1,1,2,2-tetrachloroethane	75.75/6.54	10′

Table 3 $^{1}H–^{1}H$ cross-correlations between nonequivalent protons observed from the TOCSY spectrum

Cross-correlation peak No.	Coupled protons		Cross-correlation peak position (ppm)
	Proton I	Proton II	
I	CH_3 of hexane	CH_2 of hexane	0.83/1.22
II	CH_3 of $–CO_2CH_2CH(CH_3)_2$	CH of $–CO_2CH_2CH(CH_3)_2$	0.94/1.97
III	CH_3 of $–CO_2CH_2CH(CH_3)_2$	CH_2 of $–CO_2CH_2CH(CH_3)_2$	0.94/4.01
IV	CH_3 of ethanol	CH_2 of ethanol	1.15/3.60
V	CH_3 of $–CO_2CH_2CH_3$	CH_2 of $–CO_2CH_2CH_3$	1.30/4.28
VI	CH of $–CO_2CH_2CH(CH_3)_2$	CH_2 of $–CO_2CH_2CH(CH_3)_2$	1.97/4.01

observed from the NMR and HPLC analysis that $–CO_2CH_2CH_3$ and DEP concentration increases approximately two times (Table 1).

3.4 $MgCl_2$ Structural Studies

High catalytic productivity requires active $MgCl_2$, characterized by small crystallites of $MgCl_2$ resulting in high surface area available to donors and $TiCl_4$ to bind. The (104) and (110) lateral cuts of active $MgCl_2$ having unsaturated Mg ions act as Lewis acid sites for coordination with titanium chloride fragments for active sites' formation and have high surface energy and chemically unstable.

Figure 7 is showing the deconvoluted WAXD of Catalyst-1 with the following features: broad peaks at 2θ 9–18°, 27–38° and 48–54°, broad halo at 2θ 21, 43 and 57–67°. Crystallite width calculated from the diffraction peak at 50.3 2θ is 45 Å. Deconvolution of the WAXD profile was done to study the presence of different phases of $MgCl_2$ [26, 32, 33]. The deconvoluted WAXD profile is indicative of the α-form having cubic closed packing (ccp) and β-form of $MgCl_2$ having hexagonal closed packing (hcp) and distorted δ-form of $MgCl_2$. Similar characteristics were

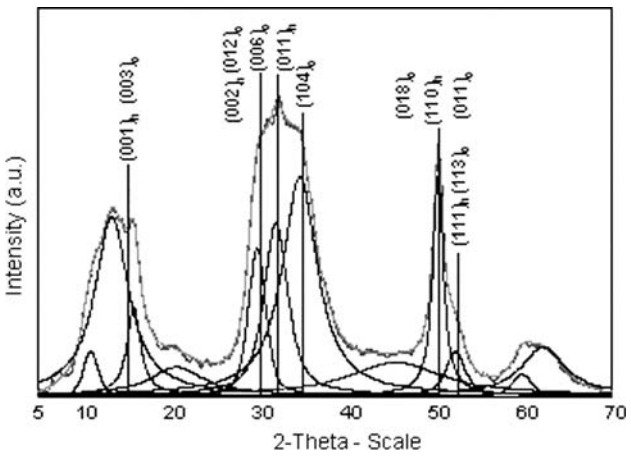

Fig. 7 Deconvoluted WAXD profile of Catalyst-1, planes corresponding to α-form having ccp have been indicated by the *subscript* '*c*' and planes corresponding to β-form having hcp have been indicated by the *subscript* '*h*'

observed for Catalyst-2 and Catalyst-3 with crystallite size of 47 and 45 Å, respectively. The broad peaks and small crystallite width is representative of small crystallites and highly disordered structure providing high surface area for high catalytic productivity.

3.5 Propylene Polymerization Performance

Catalysts were evaluated for propylene polymerization performance at high pressure. Catalyst-1 showed productivity of 6.5 kg PP g^{-1} catalyst with ~96% isotacticity index. Catalyst-2 and Catalyst-3 showed lower productivity of 5.1 and 4.8, respectively, with ~95% isotacticity index. Catalyst-1 showed higher productivity with similar isotacticity index in comparison to Catalyst-2 and Catalyst-3. The reasons for higher productivity for Catalyst-1 can be (1) higher concentration of internal donors (DIBP, DEP) (2) these bidentate donors provide stability to the active sites during polymerization [26] and (3) phthaloyl chloride present in higher concentration in Catalyst-2 is not good internal donor. The synergistic effect of these factors lowers down the productivity of Catalyst-2 and Catalyst-3.

4 Conclusions

In the present study, DIBP based high performance $MgCl_2$ supported titanium catalysts were synthesized and observed to consist of a complex mixture of organic components. Catalyst characterization using FTIR, NMR and HPLC revealed the presence of diethyl phthalate, isobutylethyl phthalate and phthaloyl chloride along with DIBP as the main organic component. Comprehensive assignment of ^{1}H and $^{13}C\{^{1}H\}$ NMR spectra was done using 2D ^{1}H–^{1}H and ^{1}H–^{13}C correlation spectroscopy. Reaction pathway for the synthesis of diethyl phthalate, isobutylethyl phthalate and phthaloyl chloride was substantiated. Productivity of catalysts with higher amount of phthaloyl chloride species was observed to be lower with similar isotacticity index. This indicate that as the isotacticity index remains the same nature of active sites remain the same, but overall concentration of active sites is reduced and protection to the active sites gets reduced with decrease in concentration of phthalate esters.

References

1. Barbe C, Cecchin G, Noristi L (1987) Adv Polym Sci 81:1
2. Corradini P (2004) J Polym Sci A Polym Chem 42:391
3. Galli P, Vecellio G (2004) J Polym Sci A Polym Chem 42:396
4. Correa A, Piemontesi F, Morini G, Cavallo L (2007) Macromolecules 40:9181
5. Busico V, Causa M, Cipullo R, Credendino R, Cutillo F, Friederichs N, Lamanna R, Segre A, Castelli VVA (2008) J Phys Chem C 112:1081
6. Cheng HN (1993) Macromol Theory Simul 2:901
7. Cavallo L, Guerra G, Corradini P (1998) J Am Chem Soc 120:2428
8. Busico V, Cipullo R, Monaco G, Vacatello M, Segre AL (1997) Macromolecules 30:6251
9. Busico V, Cipullo R (2001) Prog Polym Sci 26:443
10. Chadwick JC, van der Burgt FPTJ, Rastogi S, Busico V, Cipullo R, Talarico G, Heere JJR (2004) Macromolecules 37:9722
11. Kim SH, Somorjai GA (2001) J Phys Chem B 105:3922
12. Albizzati E, Giannini U, Morini G, Galimberti M, Barino L, Scordamaglia R (1995) Macromol Symp 89:73
13. Soga K, Park JR, Shiono T (1990) Makromol Chem Rapid Commun 11:117
14. Ferreira ML, Damiani DE (1999) J Mol Catal A Chem 150:53
15. Cecchin G, Morini G, Pelliconi A (2001) Macromol Symp 173:195
16. Galli P (1995) Macromol Symp 89:11
17. Gupta VK (1999) J Polym Mater 16:97
18. Chadwick JC (2001) Macromol Symp 173:21
19. Ribour D, Monteil V, Spitz R (2008) J Polym Sci A Polym Chem 46:5461
20. Andoni A, Chadwick JC, Milani S, Niemantsverdriet HJW, Thüne PC (2007) J Catal 247:129
21. Andoni A, Chadwick JC, Niemantsverdriet HJW, Thüne PC (2007) Macromol Rapid Commun 28:1466
22. Mori H, Sawada M, Higuchi T, Hasebe K, Otsuka N, Terano M (1999) Macromol Rapid Commun 20:245
23. Andoni A, Chadwick JC, Niemantsverdriet HJW, Thüne PC (2008) J Catal 257:81
24. Noto VD, Fregonese D, Marigo A, Bresadola S (1998) Macromol Chem Phys 199:633
25. Vittadello M, Stallworth PE, Alamgir FM, Suarez S, Abbrent S, Drain CM, Noto VD, Greenbaum SG (2006) Inorg Chim Acta 359:2513
26. Singh G, Kaur S, Makwana U, Patankar RB, Gupta VK (2009) Macromol Chem Phys 210:69
27. Yang CB, Hsu CC, Park YS, Shurvell HF (1994) Eur Polym J 30:205
28. Potapov AG, Bukatov GD, Zakharov VA (2006) J Mol Catal A Chem 246:248
29. Kissin YV, Liu X, Pollick DJ, Brungard NL, Chang M (2008) J Mol Catal A Chem 287:45
30. Ikeuchi H, Yano T, Ikai S, Sato H, Yamashita J (2003) J Mol Catal A Chem 193:207
31. Gupta VK, Satish S, Bhardwaj IS (1994) J Macromol Sci A Pure Appl Chem 31:451
32. Hu Y, Chien JCW, Polym J, Sci A (1988) Polym Chem 26:2003
33. Chein JCW, Wu JC, Kuo CI (1983) J Polym Sci A Polym Chem 21:737